Fermi National Accelerator Laboratory

FERMILAB-Conf-91/53-A
February 1991

CAN NON-GAUSSIAN FLUCTUATIONS FOR STRUCTURE FORMATION ARISE FROM INFLATION?

D.S. Salopek
NASA/ Fermilab Astrophysics Center
P.O. Box 500 MS-209
Batavia, Illinois, USA 60510

ABSTRACT

Non-Gaussian fluctuations for structure formation may be generated during the inflationary epoch from the nonlinear interaction of two scalar fields with gravity. Semi-analytical calculations are given describing nonlinear long wavelength evolution in 3+1 dimensions. Long wavelength fields are governed by a single equation, the separated Hamilton-Jacobi equation (SHJE). I discuss complete analytic solutions of the SHJE for two scalar fields with a potential whose logarithm $\ln V(\phi_j)$ is linear. More complicated potential surfaces may be approximated by continuously joining various linear $\ln V(\phi_j)$ potentials. Typically, non-Gaussian fluctuations arise when one passes over several sharp ridges in the potential surface. One can input this richer class of initial conditions into N-body codes to see the effects on the large scale structure in the Universe. The cleanest test of non-Gaussian fluctuations will hopefully occur in the near future from large angle microwave background anisotropy experiments.

in Proceedings of the NATO Advanced Research Workshop:
Observational Tests of Inflation
Durham, England, December 10-14, 1990
ed. T. Shanks, Kluwer Academic Publishers.

Operated by Universities Research Association Inc. under contract with the United States Department of Energy

A complete solution which depends on two arbitrary parameters, b, m is,

$$H(\phi_1,\phi_2;p,\theta;b,m)=\left(\frac{8\pi V_0}{3m_p^2}\right)^{1/2}\sqrt{\frac{(3p)(m^2+1)}{m^2(3p-1)+3p}}\exp\left[-\sqrt{\frac{4\pi}{p}}\frac{(-\phi_1\sin\theta+\phi_2\cos\theta)}{m_p}\right]\cosh(u) \tag{2.7a}$$

where u is a function of b, m, ϕ_1 and ϕ_2 which is defined implicitly through,

$$\frac{\sqrt{12\pi}}{m_p}\left[(\cos\theta-m\sin\theta)\phi_2-(m\cos\theta+\sin\theta)\phi_1-b\right]=-\frac{\sqrt{3p}}{3p-1}\times$$
$$\left[u\sqrt{m^2(3p-1)+3p}+\ln\left|\cosh(u)-\sinh(u)\sqrt{m^2(3p-1)+3p}\right|\right]. \tag{2.7b}$$

All solutions of the SHJE with potential (2.6) may be derived from eq.(2.7). Surfaces of constant Hubble parameter are plotted as solid curves in Fig.(1) for the case $m=1$, $\theta=0$. The family of orthogonal lines are the physical trajectories. This solution of the SHJE may be verified by differentiation; it is actually derived by looking for symmetries in the SHJE.

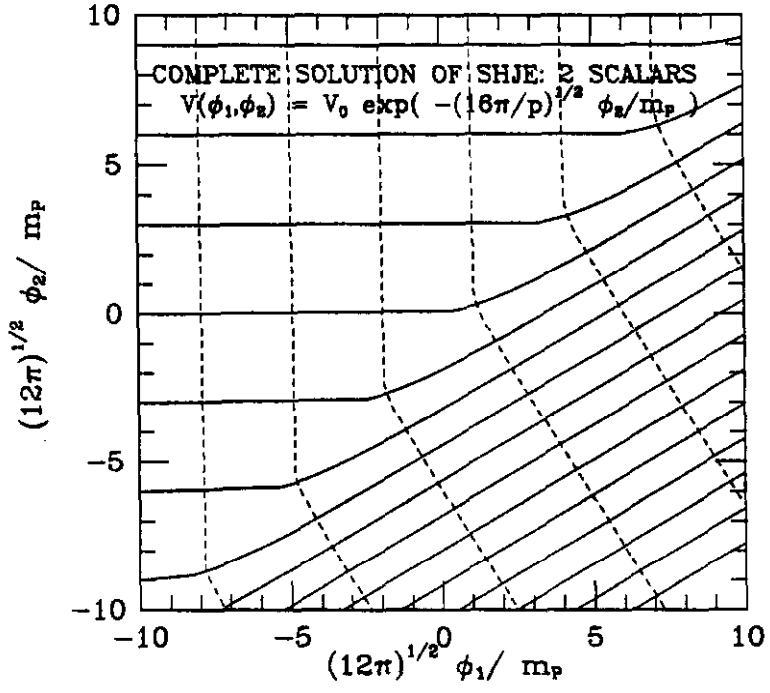

Fig. (1): The complete solution, $H(\phi_j;b,m;p,\theta)$, of the separated Hamilton-Jacobi equation is shown for two scalar fields interacting through a linear $\ln V$ potential, eq.(2.6). Here, the mixing angle θ vanishes, and the constant parameters are chosen to be $b=0$ and $m=1$. Surfaces of constant potential are just horizontal lines. The broken lines are trajectories of the fields, which are orthogonal to the surfaces of constant Hubble parameter (solid lines). One can ask what happened to space and time coordinates in the SHJE (2.4)? Loosely speaking, α, which enters in the canonical transformation (2.8) is the most natural time parameterization of the trajectories. The new canonical variables, b, m, π^b, π^m then serve as the spatial coordinates because they have no time dependence. In this sense, the Hamilton-Jacobi formalism yields the the choice of coordinates, both temporal and spatial, in which the evolution appears simplest.

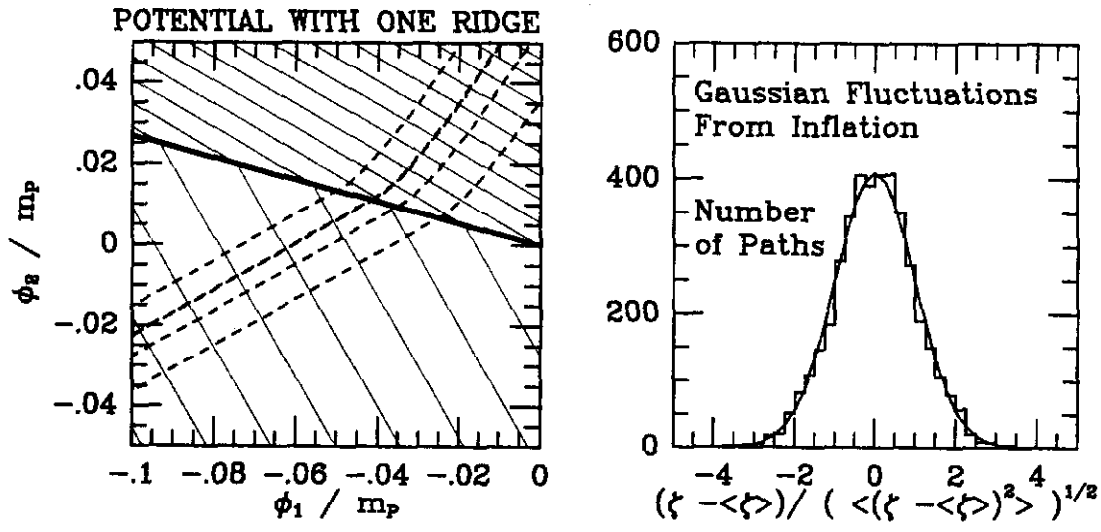

Fig. (2): (a) Some trajectories in field space are shown for a potential with a single ridge. The solid curves are lines of uniform potential, whereas the very heavy line is the ridge. The trajectories (broken lines) begin in the lower half plane with Gaussian initial conditions generated from short wavelength quantum noise. Even when they pass over the ridge, the nonlinear metric fluctuation ζ still remains Gaussian distributed, as shown in the histogram of Fig.(b) which displays the results of a 64^3 lattice simulation.

Fig. (3): (a) Non-Gaussian fluctuations consistent with CMB limits may be generated when one passes over several ridges in the potential. The light solid curves are lines of uniform potential, whereas the heavy lines are the ridges. If the scalar field trajectories (broken lines) pass sufficiently near the origin, nonlinear effects at long wavelengths are important. For a 64^3 lattice simulation, the histogram of resulting microwave background fluctuations at large angular scales ($\Delta T_{CMB}/T_{CMB} = \zeta/15$) is shown in Fig.(b). For comparison, a Gaussian distribution (smooth curve) with the same mean and dispersion as the histogram is also shown.

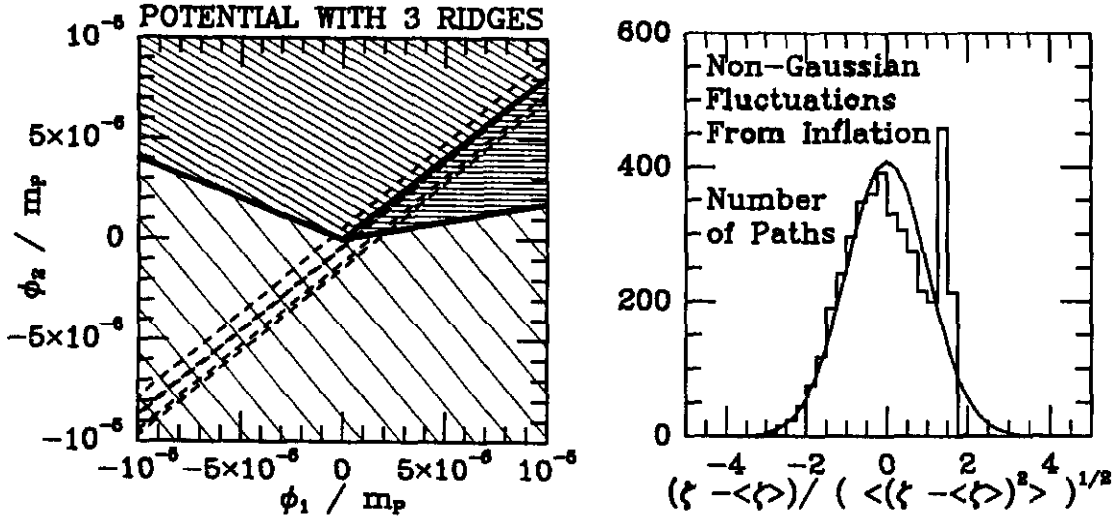

Fermi National Accelerator Laboratory

FERMILAB-Conf-91/53-A
February 1991

CAN NON-GAUSSIAN FLUCTUATIONS FOR STRUCTURE FORMATION ARISE FROM INFLATION?

D.S. Salopek
NASA/ Fermilab Astrophysics Center
P.O. Box 500 MS-209
Batavia, Illinois, USA 60510

ABSTRACT

Non-Gaussian fluctuations for structure formation may be generated during the inflationary epoch from the nonlinear interaction of two scalar fields with gravity. Semi-analytical calculations are given describing nonlinear long wavelength evolution in 3+1 dimensions. Long wavelength fields are governed by a single equation, the separated Hamilton-Jacobi equation (SHJE). I discuss complete analytic solutions of the SHJE for two scalar fields with a potential whose logarithm $\ln V(\phi_j)$ is linear. More complicated potential surfaces may be approximated by continuously joining various linear $\ln V(\phi_j)$ potentials. Typically, non-Gaussian fluctuations arise when one passes over several sharp ridges in the potential surface. One can input this richer class of initial conditions into N-body codes to see the effects on the large scale structure in the Universe. The cleanest test of non-Gaussian fluctuations will hopefully occur in the near future from large angle microwave background anisotropy experiments.

in Proceedings of the NATO Advanced Research Workshop:
Observational Tests of Inflation
Durham, England, December 10-14, 1990
ed. T. Shanks, Kluwer Academic Publishers.

Operated by Universities Research Association Inc. under contract with the United States Department of Energy

1. INTRODUCTION

Although inflation predicts that $\Omega = 1$, it does not give a unique prediction for the primordial fluctuations for structure formation. The simplest inflation models utilizing a single scalar field yield a flat fluctuation spectrum for the Newtonian potential with Gaussian distributed Fourier amplitudes. Here, however, I discuss stochastic inflation calculations (see, for example, Salopek and Bond[1]) describing non-Gaussian primordial fluctuations. The models presented may shed some light on the problems of large scale structure in the Universe.[2] Hopefully, cosmic microwave background (CMB) anisotropy experiments[3] will provide the most definitive tests of these scenarios.

In this report, I will not use the full stochastic machinery. I will assume that the fluctuations for structure formation leave the horizon when the value of the Hubble parameter is much smaller than the Planck scale. In addition, it will be assumed that the potential does not change rapidly at that time. I will consider only models where nonlinear effects become important later when all scales of cosmological interest are very much larger than the Hubble radius. Different comoving points are then no longer in causal contact, and the analysis is tractable.

Quite remarkably, the full nonlinear dynamics of long wavelength fields is contained in a single equation, the separated Hamilton-Jacobi equation (SHJE) which is a radical starting point for numerical calculations in general relativity. It is useful for several reasons. The equation is truly covariant in that it makes no reference to either the time parameter nor to the spatial coordinates. When one performs calculations, it is not necessary to make any gauge choice. The Hubble parameter is calculated in field space, $H \equiv H(\phi_k)$ rather than on a spatial lattice. Loosely speaking, the determinant of the 3-metric is the natural time parameter because it separates from the full Hamilton-Jacobi equation. The new canonical variables may actually be taken to be the spatial coordinates because they are constants along comoving spatial points.

For multiple scalar fields, the method of calculation is based on some analytic tricks rather than brute force numerics. If the logarithm of the potential for multiple scalar fields is linear, one can obtain a complete solution of the SHJE by utilizing hidden symmetries.[4] More complicated potential surfaces can be modelled by continuously matching linear $\ln V$ potentials along straight line boundaries. In fact, one can construct viable non-Gaussian models consistent with current CMB limits if one employs a potential with three ridges.[5]

2. LONG WAVELENGTH EQUATIONS

Given some initial conditions, it will be shown how to solve for the long wavelength evolution of scalar fields $\phi_j(t, x)$ with potential $V(\phi_j)$ interacting through gravity. It will be assumed that the metric has the form,

$$ds^2 = -N^2(t,x)dt^2 + e^{2\alpha(t,x)}((dx^1)^2 + (dx^2)^2 + (dx^3)^2), \qquad (2.1)$$

which describes an isotropic Universe with inhomogeneous scale factor $e^{\alpha(t,x)}$. The lapse function N is determined when one decides the time hypersurface, although an explicit choice is not necessary. Gravitational radiation has been neglected which is typically an excellent approximation, although its evolution, too, is tractable if one employs the powerful machinery of canonical transformations.[4] In what follows, $H(t,x) \equiv \dot{\alpha}/N$ is the Hubble parameter and $\pi^{\phi_j}(t,x) = e^{3\alpha}\dot{\phi}_j/N$ are the momentum densities of the scalar fields.

All second order spatial gradients in the Lagrangian of Einstein gravity with scalar fields will be neglected, but it is necessary to retain first order spatial gradients otherwise one returns to homogeneous minisuperspace. The energy constraint,

$$H^2 = \frac{8\pi}{3m_p^2}\left[\frac{e^{-6\alpha}}{2}\sum_j \pi^{\phi_j}{}^2 + V(\phi_j)\right], \tag{2.2a}$$

and the evolution equations are valid at each comoving spatial point, and they are the same as those for homogeneous flat cosmologies. The new ingredient is the momentum constraint, which joins together the independent spatial points to make one Universe:

$$H_{,i} = -\frac{4\pi}{m_p^2}\, e^{-3\alpha}\pi^{\phi_j}\phi_{j,i}. \tag{2.2b}$$

The solution of this equation is familiar to those who study fluid mechanics. The Hubble parameter is assumed to be a function of the scalar fields, and the momentum densities are given by partial derivatives with respect to the scalar fields,

$$H \equiv H(\phi_j), \qquad \pi^{\phi_j} = -\frac{m_p^2}{4\pi}e^{3\alpha}\frac{\partial H}{\partial \phi_j}. \tag{2.3}$$

When these are substituted into the energy constraint, one obtains the separated Hamilton-Jacobi equation,

$$H^2 = \frac{m_p^2}{12\pi}\sum_j\left(\frac{\partial H}{\partial \phi_j}\right)^2 + \frac{8\pi V(\phi_j)}{3m_p^2}. \tag{2.4}$$

This remarkable equation governs the nonlinear dynamics of the long wavelength gravitational system. It is covariant in that is does not refer either to the time hypersurface nor to the spatial coordinates.

In a significant improvement for calculations based on Hamilton-Jacobi methods[4] (hereafter known as S1), I gave an complete analytic solution of the SHJE for two scalar fields (ϕ_1', ϕ_2') interacting with an exponential potential,

$$V(\phi_1', \phi_2'; p) = V_0 \exp\left(-\sqrt{\frac{16\pi}{p}}\,\frac{\phi_2'}{m_p}\right). \tag{2.5}$$

The coupling parameter p controls the steepness of the potential. The SHJE for two scalar fields interacting through arbitrary linear $\ln V(\phi_1, \phi_2)$ potential,

$$V(\phi_1, \phi_2; p, \theta) = V_0 \exp\left[-\sqrt{\frac{16\pi}{p}}\,\frac{\left(-\phi_1 \sin\theta + \phi_2 \cos\theta\right)}{m_p}\right]. \tag{2.6}$$

may then be solved by rotating the fields (ϕ_1', ϕ_2') by a mixing angle θ:

$$\phi_1' = \phi_1 \cos\theta + \phi_2 \sin\theta, \qquad \phi_2' = -\phi_1 \sin\theta + \phi_2 \cos\theta, \tag{2.7}$$

A complete solution which depends on two arbitrary parameters, b, m is,

$$H(\phi_1,\phi_2;p,\theta;b,m)=\left(\frac{8\pi V_0}{3m_p^2}\right)^{1/2}\sqrt{\frac{(3p)(m^2+1)}{m^2(3p-1)+3p}}\exp\left[-\sqrt{\frac{4\pi}{p}}\frac{\left(-\phi_1\sin\theta+\phi_2\cos\theta\right)}{m_p}\right]\cosh(u) \tag{2.7a}$$

where u is a function of b, m, ϕ_1 and ϕ_2 which is defined implicitly through,

$$\frac{\sqrt{12\pi}}{m_p}\left[(\cos\theta-m\sin\theta)\phi_2-(m\cos\theta+\sin\theta)\phi_1-b\right]=-\frac{\sqrt{3p}}{3p-1}\times$$
$$\left[u\sqrt{m^2(3p-1)+3p}+\ln\left|\cosh(u)-\sinh(u)\sqrt{m^2(3p-1)+3p}\right|\right]. \tag{2.7b}$$

All solutions of the SHJE with potential (2.6) may be derived from eq.(2.7). Surfaces of constant Hubble parameter are plotted as solid curves in Fig.(1) for the case $m=1$, $\theta=0$. The family of orthogonal lines are the physical trajectories. This solution of the SHJE may be verified by differentiation; it is actually derived by looking for symmetries in the SHJE.

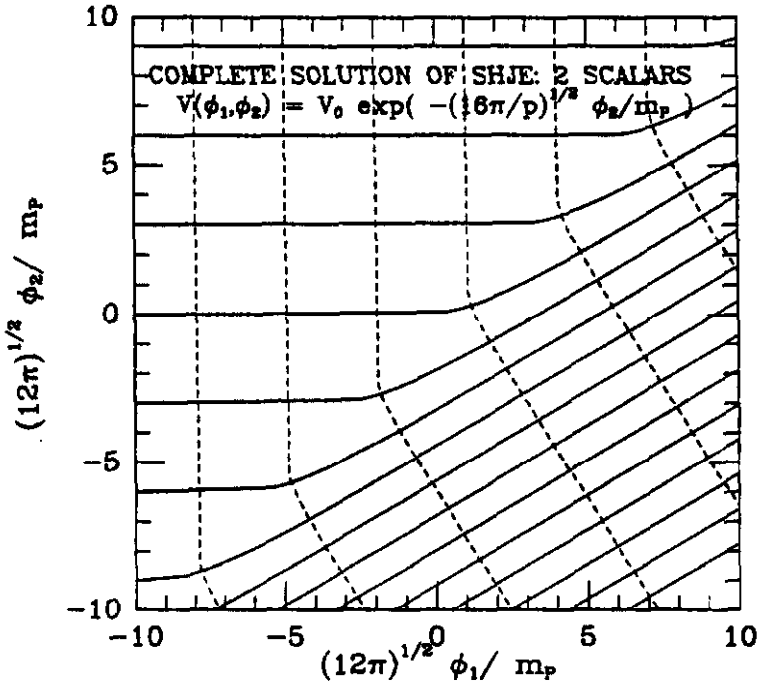

Fig. (1): The complete solution, $H(\phi_j;b,m;p,\theta)$, of the separated Hamilton-Jacobi equation is shown for two scalar fields interacting through a linear $\ln V$ potential, eq.(2.6). Here, the mixing angle θ vanishes, and the constant parameters are chosen to be $b=0$ and $m=1$. Surfaces of constant potential are just horizontal lines. The broken lines are trajectories of the fields, which are orthogonal to the surfaces of constant Hubble parameter (solid lines). One can ask what happened to space and time coordinates in the SHJE (2.4)? Loosely speaking, α, which enters in the canonical transformation (2.8) is the most natural time parameterization of the trajectories. The new canonical variables, b, m, π^b, π^m then serve as the spatial coordinates because they have no time dependence. In this sense, the Hamilton-Jacobi formalism yields the the choice of coordinates, both temporal and spatial, in which the evolution appears simplest.

The complete solution (2.7) generates a transformation to new canonical variables, b, m, with conjugate momenta, π^b and π^m, given by differentiation of the Hubble parameter,

$$\pi^b = \frac{m_p^2}{4\pi} e^{3\alpha} \frac{\partial H}{\partial b}, \qquad \pi^m = \frac{m_p^2}{4\pi} e^{3\alpha} \frac{\partial H}{\partial m}. \tag{2.8}$$

The Hamiltonian density actually vanishes strongly at each spatial point when expressed in terms of these new variables. Hence, they are constants in time, although they may be spatially dependent. Moreover, the new canonical variables are constrained through the new version of the momentum constraint,

$$0 = \pi^b b_{,i} + \pi^m m_{,i}, \tag{2.9}$$

Once may invert (2.3) and (2.8) to determine the 4 constants of integration as a function of the original variables, α, ϕ_j, π^{ϕ_j}:

$$b \equiv b(\alpha, \phi_j, \pi^{\phi_j}; p, \theta), \quad \text{and similarly for } m, \pi^b, \pi^m. \tag{2.10}$$

These complicated analytic expressions are explicitly given in S1, and they will play a crucial role in what follows. In terms of the new canonical variables,[4] one may write an explicit analytic expression for the variable ζ which characterizes adiabatic fluctuations at long wavelengths,[6]

$$\zeta \equiv \zeta(b, m, \pi^b, \pi^m; p, \theta). \tag{2.11}$$

It is the quantity of primary interest for the simplest models of structure formation. For example, in the Cold Dark Matter Model, microwave background anisotropies at angular scales greater than $\sim 3^0$ are directly proportional to it, $\Delta T_{CMB}/T_{CMB} = \zeta/15$.

3. INITIAL CONDITIONS

In Sec. 4, models are constructed by joining several linear $\ln V$ potentials together. It will be assumed that *Gaussian* fluctuations arising from short wavelength quantum noise are generated in region 1 where the potential parameters are p_1 and θ_1. Non-Gaussian fluctuations are produced when one passes over other regions of the potential.

The Hubble function, $H(\phi_j)$, in region 1 is taken to be the attractor solution,

$$H_{att}(\phi_j) = \sqrt{\frac{8\pi}{3m_p^2} \frac{V_0}{1 - 1/(3p_1)}} \exp\Big[- \sqrt{\frac{4\pi}{p_1}} \frac{(-\phi_1 \sin\theta_1 + \phi_2 \cos\theta_1)}{m_p} \Big] \tag{3.1}$$

corresponding to $b = -\infty$ and $m = 0$ in (2.7) having homogeneous values. The new momentum constraint (2.9) is then satisfied at early times, and the evolution equations guarantee that it will be satisfied at late times. In region 1, the fields then evolve in time α according to,

$$\phi_1(x, \alpha) = -\frac{m_p}{\sqrt{4\pi p_1}} \alpha \sin\theta_1 + \phi_{10}(x), \quad \phi_2(x, \alpha) = \frac{m_p}{\sqrt{4\pi p_1}} \alpha \cos\theta_1 + \phi_{20}(x), \tag{3.2a}$$

$$\pi^{\phi_1}(x, \alpha) = -\frac{m_p}{\sqrt{4\pi p_1}} e^{3\alpha} H_{att}(\phi_j) \sin\theta_1, \quad \pi^{\phi_2}(x, \alpha) = \frac{m_p}{\sqrt{4\pi p_1}} e^{3\alpha} H_{att}(\phi_j) \cos\theta_1. \tag{3.2b}$$

The initial values of the scalar fields, $\phi_{i0}(x)$, are classical Gaussian random fields with power spectrum

$$\mathcal{P}_{\phi_{i0}}(k) \equiv \frac{k^3}{2\pi^2}|\phi_{i0}(k)|^2 = \left(\frac{H_0}{2\pi}\right)^2 \left(\frac{k}{H_0 e^{\alpha_0}}\right)^{-2/(p_1-1)}.$$

The amplitudes of the homogeneous $k = 0$ modes are arbitrary. If the value of the Hubble parameter, H_0, when the longest modes in the simulation left the horizon during inflation, is much smaller than the Planck scale then the assumption of Gaussian initial conditions is justified. I will not give the full lattice results[5] here; I will show only the $\Delta T_{CMB}/T_{CMB}$ distribution at large angular scales.

4. MODEL CALCULATIONS

Two sets of calculations will be given. For illustration purposes, I will describe in detail a potential with a single ridge although it generically produces Gaussian fluctuations. When there are three ridges in the potential, then one can indeed generate non-Gaussian fluctuations.

4.1 POTENTIAL WITH A RIDGE

Consider a potential obtained by joining two linear $\ln V$ potentials continuously along the line $\phi_2 = \phi_1 \tan\chi_{12}$ (see Fig.(2a)). Continuity of the potential at the boundary implies that the potential parameters, p_2 and θ_2 in the upper half-plane (region 2), are related to those in the upper half (region 1) through,

$$\sqrt{\frac{p_2}{p_1}} = \frac{\sin(\chi_{12}-\theta_2)}{\sin(\chi_{12}-\theta_1)}. \tag{4.1}$$

For a given spatial point in the lattice, the value of the fields at the interface follow from (3.2),

$$\alpha_I = \frac{\sqrt{4\pi p_1}}{m_p}\frac{(\phi_{10}\sin\chi_{12} - \phi_{20}\cos\chi_{12})}{\cos(\chi_{12}-\theta_1)}, \tag{4.2a}$$

$$\phi_{1I} = \frac{\cos\chi_{12}}{\cos(\chi_{12}-\theta_1)}\left(\phi_{10}\cos\theta_1 + \phi_{20}\sin\theta_1\right), \quad \phi_{2I} = \frac{\sin\chi_{12}}{\cos(\chi_{12}-\theta_1)}\left(\phi_{10}\cos\theta_1 + \phi_{20}\sin\theta_1\right), \tag{4.2b}$$

$$\pi_I^{\phi_1} = -\frac{m_p}{\sqrt{4\pi p_1}} H_{att}(\phi_{1I},\phi_{2I})\, e^{3\alpha_I}\sin\theta_1, \quad \pi_I^{\phi_2} = \frac{m_p}{\sqrt{4\pi p_1}} H_{att}(\phi_{1I},\phi_{2I})\, e^{3\alpha_I}\cos\theta_1. \tag{4.2c}$$

Using these values, one can determine the constants of integration (2.10) in region 2, and then calculate ζ, eq.(2.12), which yields the CMB temperature anisotropy at large angular scales. All the equations are algebraic.

In Fig.(2a), I show the potential as well as some typical trajectories. In Fig.(2b), I show the distribution of ζ on a 2-D slice from a 64^3 lattice calculation. For plotting purposes, the initial value of the Hubble parameter was chosen to be $H_0 = 10^{-2}m_p$, although microwave background anisotropy limits would require $H_0 < 10^{-4}m_p$. Here, the potential parameters in the lower half-plane are $p_1 = 20$, $\theta_1 = -60$; in the upper half-plane, $\theta_2 = -30^0$. The ridge is inclined at an angle of $\chi_{12} = 165^0$ to the ϕ_1 axis. Surprisingly, one still obtains Gaussian statistics (Fig.(2b)) although the fields mix at the interface. For a potential with

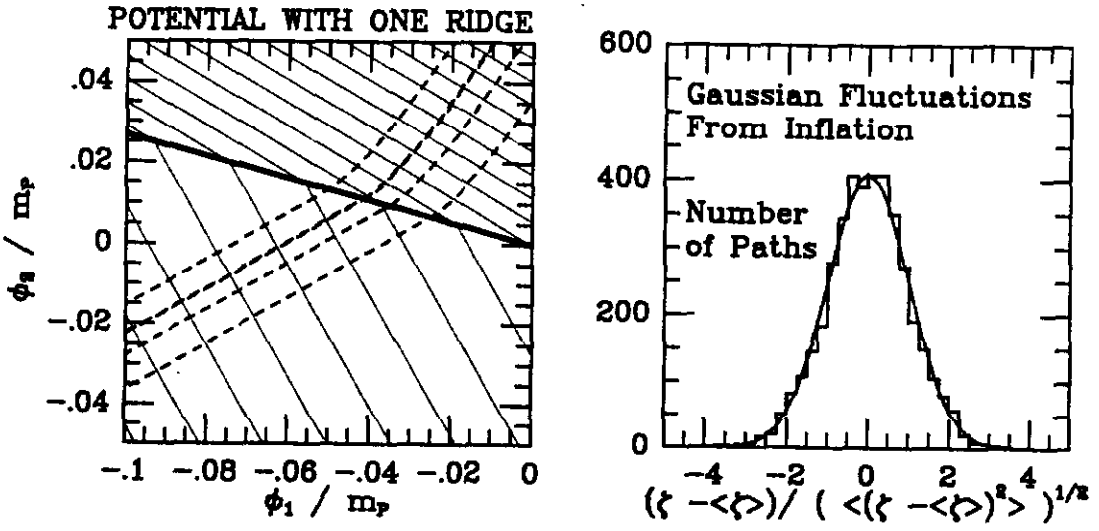

Fig. (2): (a) Some trajectories in field space are shown for a potential with a single ridge. The solid curves are lines of uniform potential, whereas the very heavy line is the ridge. The trajectories (broken lines) begin in the lower half plane with Gaussian initial conditions generated from short wavelength quantum noise. Even when they pass over the ridge, the nonlinear metric fluctuation ζ still remains Gaussian distributed, as shown in the histogram of Fig.(b) which displays the results of a 64^3 lattice simulation.

Fig. (3): (a) Non-Gaussian fluctuations consistent with CMB limits may be generated when one passes over several ridges in the potential. The light solid curves are lines of uniform potential, whereas the heavy lines are the ridges. If the scalar field trajectories (broken lines) pass sufficiently near the origin, nonlinear effects at long wavelengths are important. For a 64^3 lattice simulation, the histogram of resulting microwave background fluctuations at large angular scales ($\Delta T_{CMB}/T_{CMB} = \zeta/15$) is shown in Fig.(b). For comparison, a Gaussian distribution (smooth curve) with the same mean and dispersion as the histogram is also shown.

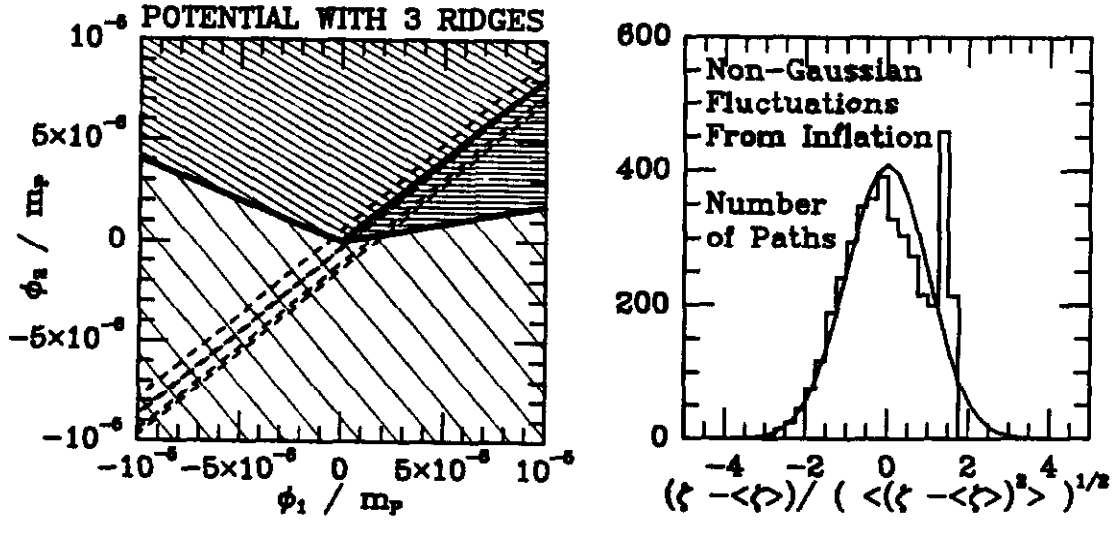

a single ridge, this result may be proved quite generally. Apparently, each trajectory evolves in a self-similar way.

4.2 POTENTIAL WITH THREE RIDGES

One can obtain non-Gaussian fluctuations on cosmologically observable scales from a potential created by joining three linear $\ln V$ regions as shown in Fig.(3). Trajectories begin in the lower half-plane, region 1 ($p_1 = 20$, $\theta_1 = -50^0$), with initial Hubble parameter, $H_0 = 10^{-6} m_P$, chosen to satisfy CMB limits. If the trajectories pass into the upper right hand area, region 2 ($\theta_2 = 0^0$), they receive an upward kick from the potential, which forces them into region 3 ($\theta_3 = -30^0$). (If this diagram were extended, one would find that trajectories actually cross in region 3.) The angles of the ridges starting with the lower right and proceeding counterclockwise are, $\chi_{12} = 10^0$, $\chi_{23} = 39^0$, and $\chi_{31} = 158^0$. The calculations here are more complicated than in Sec. 4.1 because one must determine where a trajectory strikes region 3 after it has passed through region 2. ζ is not constant in passing through region 2. The distribution of ζ in region 3 is plotted in Fig.(3b). For the parameters shown, it was found that non-Gaussian fluctuations can occur if the fields passed sufficiently near the origin, which can be arranged through the arbitrary choice of the homogeneous mode amplitudes in eq.(3.2). A thorough search of parameter space has yet to be made.

5. CONCLUSIONS

Because inflation probes arbitrarily small distance scales, it is quite likely that non-Gaussian fluctuations may arise from the interactions of various fields. However, the greatest obstacle is actually calculating these effects. As the first non-trivial improvement over homogeneous minisuperspace models, one should calculate nonlinear effects at long wavelengths. However, there is currently no strong evidence for non-Gaussian fluctuations.[7] The goal here then is to generate some simple models that can be used to test the non-Gaussian hypothesis with observational data. The major achievement of this report over earlier work[8-10,1,11] is an efficient way of calculating *observable* non-Gaussian models using Hamilton-Jacobi theory. (Previously, the only fully calculable non-Gaussian model consistent with microwave background limits was proposed by Bardeen[12] who considered the square of a Gaussian random field whose power spectrum peaked at cluster scales.)

In the future, the models presented here will be compared with large scale structure observations. The cleanest test of models of non-Gaussian fluctuations will hopefully come in the near future from the Cosmic Background Explorer satellite[3] which should be in a position to test the Cold Dark Matter Model prediction.[13]

I would like to thank J.R. Bond for several stimulating discussions. This work was supported by the U.S. Department of Energy and NASA at Fermilab (Grant No. NAGW-1340).

[1] Salopek, D.S. and Bond, J.R., Phys. Rev. **D42**, 3936 (1990), **D43**, 1005 (1991).

[2] Maddox, S.J., Efstathiou, G., Sutherland, W.J. and Loveday, J., Mon. Not. R. Astr. Soc., **242**, 43P (1990).

[3] Smoot, G., in these proceedings (1990).

[4] Salopek, D.S., submitted to Phys. Rev. D Fermilab-Pub-90/273-A (1990). Referred to as S1.

[5] Salopek, D.S., to be submitted to the Ap.J. (1991). Referred to as S2.

[6] Bardeen, J.M., Steinhardt, P.J. and Turner, M.S., Phys. Rev. **D28**, 670 (1983).

[7] Melott, A.L., in these proceedings (1990).

[8] Allen, T.J., Grinstein, B. and Wise, M., Phys. Lett. **B197**, 66 (1987).

[9] Matarrese, S., Ortolan, A. and Lucchin, F. Phys. Rev. **D40**, 290 (1989).

[10] Yi, I., Vishniac, E.T. and Mineshige, S., University of Texas Preprint (1990).

[11] Mollerach, S., Matarrese, S., Ortolan, A. and Lucchin, F., SISSA 143A preprint (1990).

[12] Bardeen, J.M., talk presented at *Workshop on Inflation and Exotic Cosmic Structure Formation*, Canadian Institute for Theoretical Astrophysics, Vancouver, Canada, (1990).

[13] Bond, J.R., in Proc. of *The Early Universe*, ed. W. Unruh and G. Seminoff, Dordrecht: Kluwer (1988).